High-Resolution Seismic-Reflection Image of the Chesapeake Bay Impact Structure, NASA Langley Research Center, Hampton, Virginia

By Rufus D. Catchings, David S. Powars, Gregory S. Gohn, and Mark R. Goldman

Chapter I of
**Studies of the Chesapeake Bay Impact Structure—
The USGS-NASA Langley Corehole, Hampton, Virginia, and
Related Coreholes and Geophysical Surveys**

Edited by J. Wright Horton, Jr., David S. Powars, and Gregory S. Gohn

Prepared in cooperation with the
Hampton Roads Planning District Commission,
Virginia Department of Environmental Quality, and
National Aeronautics and Space Administration Langley Research Center

Professional Paper 1688

U.S. Department of the Interior
U.S. Geological Survey

Contents

Figures

Tables

High-Resolution Seismic-Reflection Image of the Chesapeake Bay Impact Structure, NASA Langley Research Center, Hampton, Virginia

By Rufus D. Catchings,[1] David S. Powars,[2] Gregory S. Gohn,[2] and Mark R. Goldman[1]

Abstract

A 1-kilometer-long (0.62-mile-long) seismic reflection and refraction profile collected at the National Aeronautics and Space Administration (NASA) Langley Research Center, Hampton, Va., provides a detailed image of part of the annular trough of the buried, 35-million-year-old Chesapeake Bay impact structure. This profile passes within 5 meters (m; 16.4 feet (ft)) of a 635.1-m-deep (2,083.8-ft-deep), continuously cored and geophysically logged test hole at the Langley Center (the USGS-NASA Langley corehole). High-resolution seismic-reflection images (having a common-depth-point spacing of 2.5 m (8.2 ft)) of the upper 1,000 m (3,281 ft) along the seismic profile were generated by using refraction velocities and corehole sonic velocities to convert from time sections to depth sections.

Time-distance, unmigrated depth-distance, and migrated depth-distance images show lateral variations in the geologic units observed in the USGS-NASA Langley corehole. A high-amplitude reflection at 630 to 625 m (2,067 to 2,051 ft) depth on the migrated depth image correlates with the top of weathered granite (the Langley Granite) at 626.3 m (2,054.7 ft) in the Langley core. Additional high-amplitude reflections below that depth likely represent a weathering profile developed in the upper part of the granite. Diffractions on the unmigrated images suggest that the granite contains numerous inhomogeneities that may consist of mineral veins and mineralized faults and fractures, as seen in the granite cores.

Above the granite, crater unit A (minimally to moderately disturbed sands and clays of the Cretaceous Potomac Formation) is characterized by semicontinuous, horizontal and moderately inclined reflections that are broken by pervasive, subvertical, small-offset faults. Sediments of the lower beds of crater unit A below 558.1 m (1,831.0 ft) in the core have horizontal bedding and are nearly pristine. Above that depth, the upper beds of crater unit A contain thick fluidized sand intervals and fractured clay-silt beds. The contact between the granite and crater unit A is essentially horizontal on the migrated depth profile and shows minor relief produced by a few steeply dipping faults.

Above crater unit A, the lower beds of crater unit B are lithologically similar to the upper beds of crater unit A and display similar impact-generated deformation. In the migrated depth image, crater unit A and the lower beds of crater unit B are combined into one unit. A thin zone (0.3 m (1.0 ft) thick) of injected glauconitic sediment at the base of the lower beds (at 442.5 m (1,451.7 ft) depth) is the only occurrence of exotic material in the lower beds of crater unit B in the core.

The upper beds of crater unit B (above 427.7 m (1,403.3 ft) depth) are represented by discontinuous, locally weak, isolated, or inclined reflections on the migrated depth image. In the core, the upper beds of crater unit B are divided into megablocks and megablock zones that consist of fragmented sediments of the Potomac Formation. The megablocks are separated by matrix zones that consist of smaller blocks of sediments of the Potomac Formation suspended in a matrix of native disaggregated sediments of the Potomac Formation and injected, exotic disaggregated, glauconitic Upper Cretaceous and lower Tertiary marine sediments. Angular relationships and offsets of reflections across the high-relief contact between the upper beds of crater unit B and the underlying combined crater unit A and the lower beds of crater unit B suggest that the contact is a dip-slip fault locally.

Above a contact with crater unit B at a depth of 269.4 m (884.0 ft), the Exmore beds are represented by strong, continuous and discontinuous, overstepping reflections that suggest division of the Exmore into four laterally discontinuous depositional subunits. Two of these subunits are present near the Langley corehole on the seismic images and are recognized in the core (Gohn and others, this volume, chap. C). In the Langley core, the Exmore beds consist of clasts of Cretaceous and Tertiary preimpact sediments and cataclastic, shocked,

[1]U.S. Geological Survey, Menlo Park, CA 94025.
[2]U.S. Geological Survey, Reston, VA 20192.

pre-Mesozoic igneous rocks suspended in a matrix of calcareous, muddy, quartz-glauconite sand and granules that contains shocked quartz.

The dipping, truncated, and disrupted reflections within crater units A and B are interpreted to represent a 550-m-wide (1,805-ft-wide), stratabound collapse structure. This structure does not affect the underlying basement granite or the lower beds of crater unit A, nor does it affect the base of the Exmore beds above crater unit B. The collapse structure is not bounded laterally by major normal faults. Instead, structural displacements appear to be distributed among abundant short, small-offset faults and intervals of fluidized sediment. Fluidized sands above 558 m (1,831 ft) depth in crater unit A are interpreted as a low-strength zone that accommodated the widespread, late-stage, gravitational collapse of the impact structure. The proposed Langley collapse structure may be analogous to stratabound grabens in the outer zone of the Silverpit crater (North Sea).

The Exmore beds are interpreted as impact-generated, ocean-resurge deposits. The upper contact of the Exmore section is a wavy, semicontinuous reflection that may represent large bedforms produced by resurge currents or returning impact-generated tsunamis, or it may represent the unmodified blocky or hummocky top of the final Exmore debris flow. Typically continuous, nearly horizontal reflections characterize the upper Eocene to Pleistocene postimpact section of dominantly marine sediments.

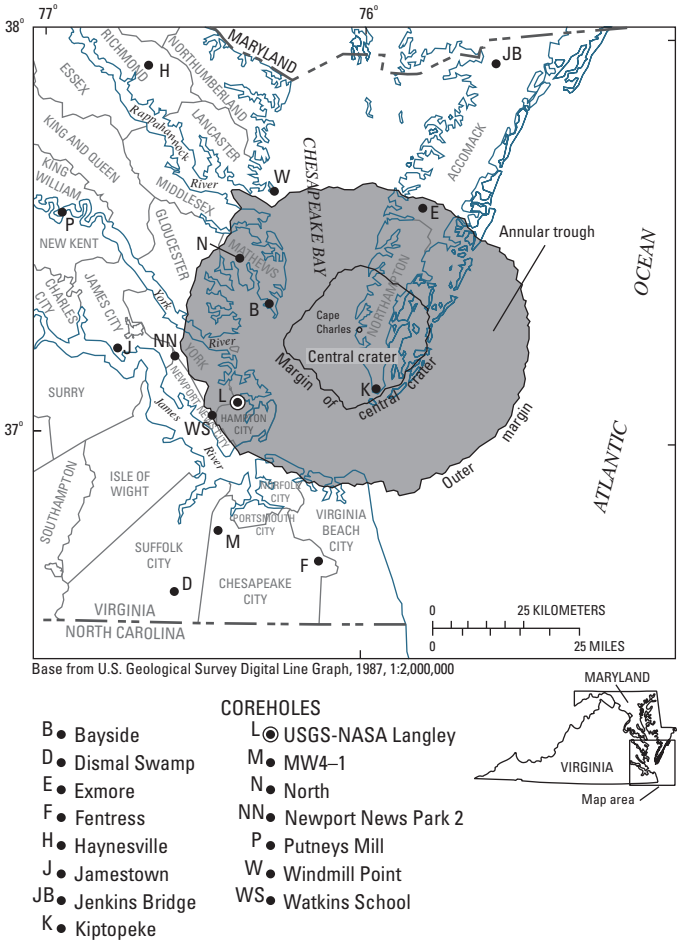

Figure I1. Regional map showing the location of the Chesapeake Bay impact structure, the USGS-NASA Langley corehole at Hampton, Va., and some other coreholes in southeastern Virginia. Locations of the central crater and outer margin are from Powars and Bruce (1999). Illustration modified from Powars, Johnson, and others (2002) and Edwards and Powars (2003).

Introduction

The Chesapeake Bay impact structure is among the largest and best preserved of the known impact craters on Earth (Poag, 1997). It is 85 kilometers (km; 53 miles (mi)) wide. This late Eocene structure lies buried beneath postimpact continental-margin sediments of the Virginia Coastal Plain and adjacent inner continental shelf (fig. I1) (Poag and others, 1994; Poag, 1997; Powars and Bruce, 1999). The center of the structure is beneath the town of Cape Charles, Va., on the Delmarva Peninsula.

Marine seismic-reflection surveys played a major role in the discovery and subsequent study of the Chesapeake Bay impact structure in the 1990s. Poag and others (1999) used over 1,200 km (746 mi) of multichannel and single-channel reflection profiles to interpret the location, major structures, and morphology of this complex crater (also see Poag and others, 1994; Poag, 1996, 1997; and Powars and Bruce, 1999). Stratigraphic and structural interpretations of the seismic profiles were substantially enhanced by the availability of stratigraphic and lithologic data from continuously cored test holes in nearby onshore areas (Powars and others, 1992; Powars and Bruce, 1999).

In 2000, the U.S. Geological Survey (USGS) and cooperating agencies (see "Acknowledgments") conducted a high-resolution seismic reflection and refraction survey and drilled a continuously cored test hole (the USGS-NASA Langley corehole) near the outer margin of the Chesapeake Bay impact structure on the York-James Peninsula (fig. I2). The objectives of these studies were to acquire the structural, stratigraphic, lithologic, petrologic, and hydrologic data needed to assess the effect of the impact structure on the regional ground-water flow regime and to infer the formative processes and geologic history of the impact structure (Gohn, Bruce, and others, 2001).

The seismic survey traversed the southern York-James Peninsula in a northeast to southwest direction at a high angle to the local trend of the impact structure's outer margin (fig. I2). The survey extended from the National Aeronautics and Space Administration (NASA) Langley Research Center on the northeast through the cities of Hampton and Newport News to the James River. The full length of the survey was 13.6 km (8.5 mi); however, substantial data gaps required by the densely populated urban setting reduced the actual surveyed distance to approximately 9 km (5.6 mi). To maintain straight-line

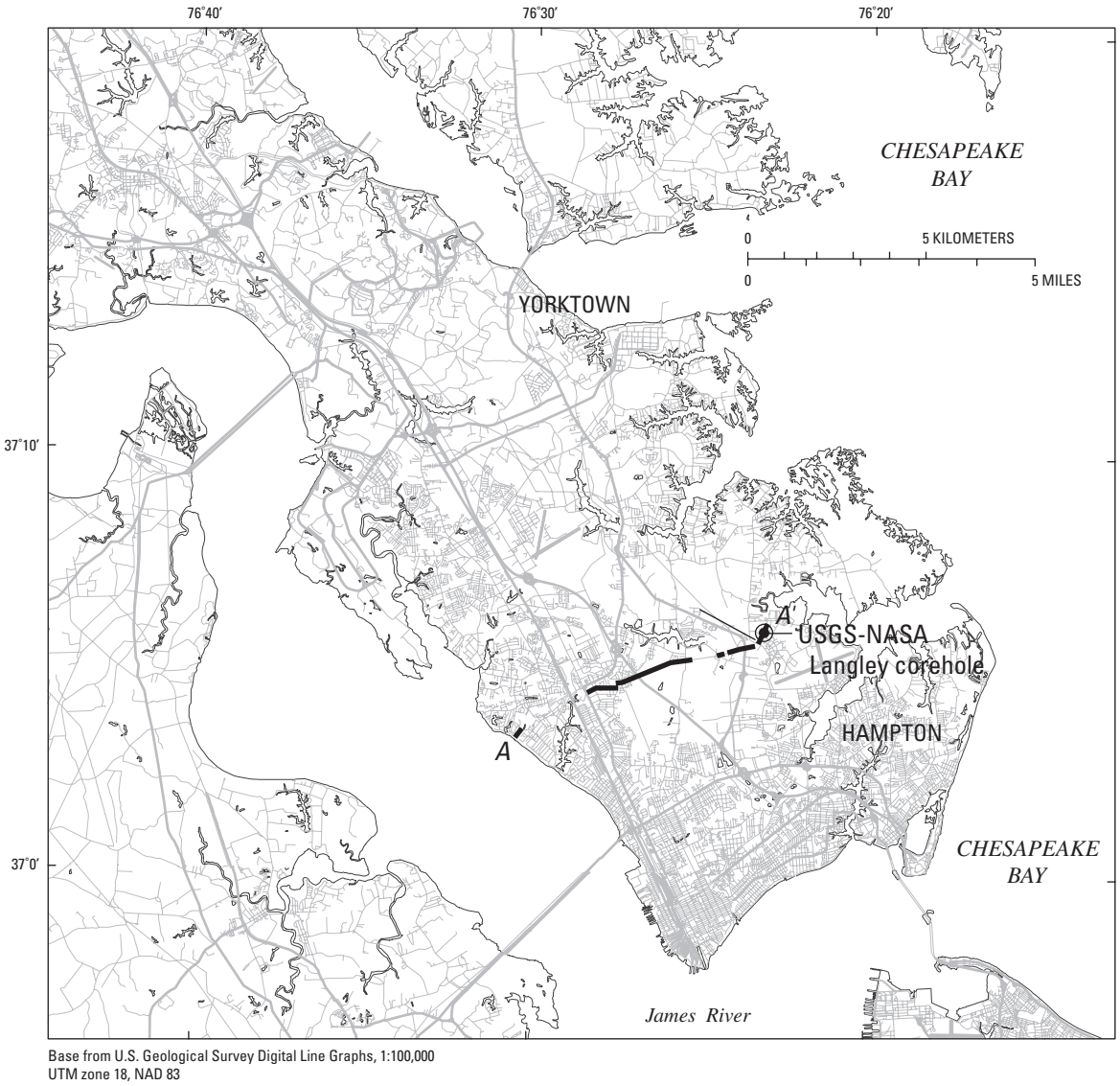

Figure I2. Map showing the location of the 1-km-long (0.62-mi-long) Langley seismic profile and the USGS-NASA Langley corehole in relation to the entire 13.6-km-long (8.5-mi-long) York-James seismic transect (*A*–*A*'). See figure I1 for the regional setting.

segments, the seismic transect was divided into nine individual seismic profiles that ranged in length from about 250 meters (m; 820 feet (ft)) to more than 2,650 m (8,694 ft, or 1.65 mi).

The USGS-NASA Langley corehole was completed to a total depth of 635.1 m (2,083.8 ft) at the NASA Langley Research Center (Gohn, Clark, and others, 2001; Powars and others, 2001). The corehole penetrated the full thickness of postimpact, impact-generated, and impact-modified sediments and bottomed in underlying granite (fig. I3). A single-transmitter, dual-receiver sonic tool was run the full length of the Langley corehole to record acoustic interval-transit times. The resulting sonic log provided much of the velocity information that was used to process the seismic-reflection data.

Core and geophysical-log depths originally were recorded in feet at the drill site. Core and log depths given in meters in this chapter are calculated from the corresponding measured depths in feet and are correlated with the seismic data, which were acquired in metric units.

This chapter presents a stratigraphic and structural interpretation of a 1-km-long (0.62-mi-long), seismic reflection and refraction profile surveyed across the NASA Langley Research Center (fig. I2). This survey passed through the Langley drill site within 5 m (16.4 ft) of the corehole, thereby providing the opportunity to integrate the core geologic data and corehole geophysical data with the seismic data. The Langley seismic profile is the northeasternmost segment of the 13.6-km-long (8.5-mi-long) York-James seismic survey.

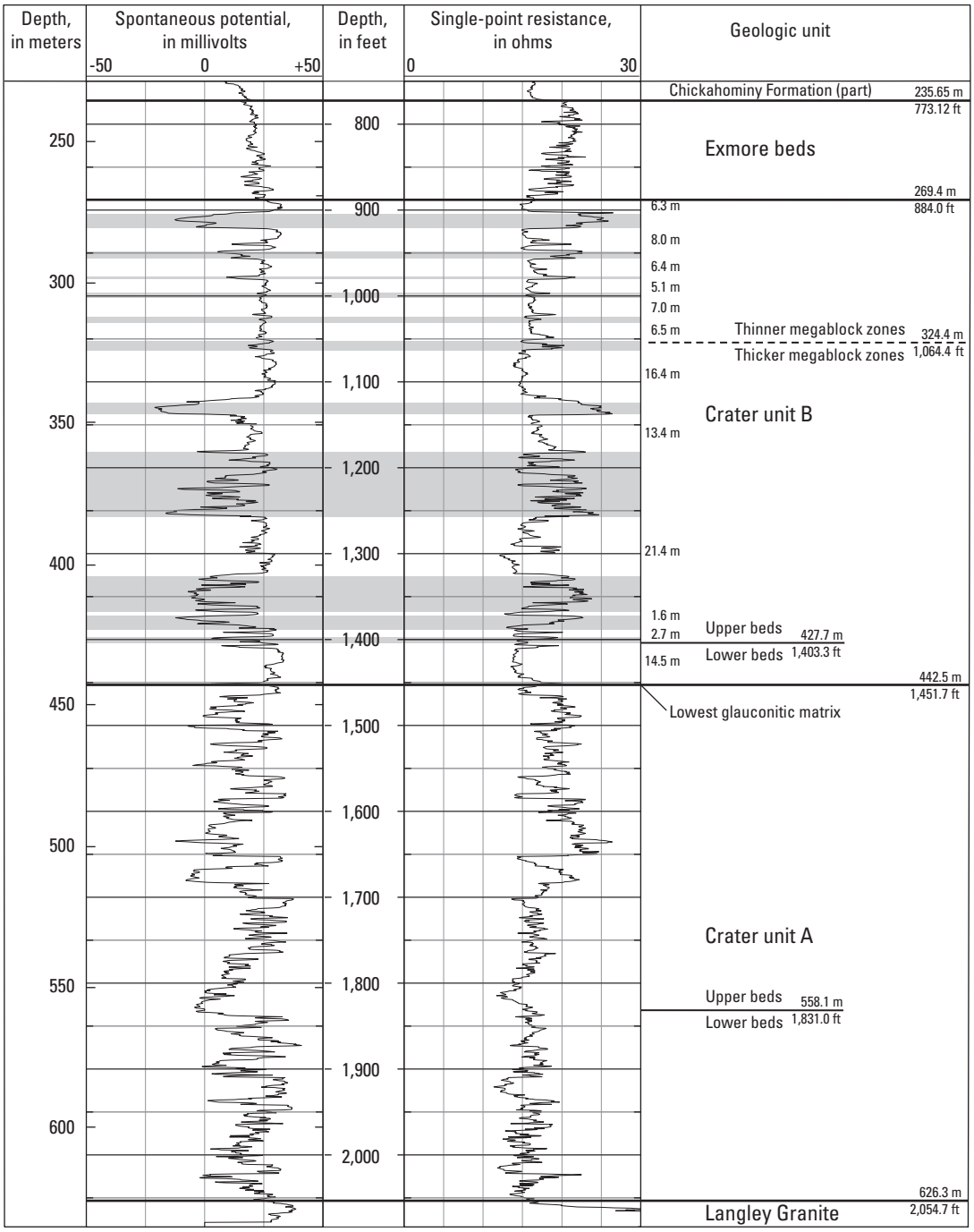

Figure I3. Summary geologic column and geophysical logs for the impact-modified sediments (crater units A and B) and impact-generated sediments (Exmore beds) in the USGS-NASA Langley core. Thicknesses of sediment megablocks in crater unit B are indicated. Shaded intervals are zones of injected glauconitic matrix in crater unit B. Figure from Gohn and others (this volume, chap. C, figs. C4 and C7).

Chesapeake Bay Impact Structure

The Chesapeake Bay impact structure is a complex crater developed in a multilayered marine target (Poag and others, 1994, 1999; Poag, 1997; Powars and Bruce, 1999; Powars, 2000). It was formed about 35 million years ago by the impact of a comet fragment or asteroid on the late Eocene continental shelf (fig. I1). Target materials below the atmosphere included an oceanic water column (<340 m (<1,115 ft) deep), a seaward-thickening Cretaceous and lower Tertiary sedimentary section (about 400 m to about 1,500 m (about 1,300 ft to about 4,900 ft) thick), and an underlying basement of igneous and metamorphic rocks (Poag, 1997; Powars and Bruce, 1999; Gohn and others, this volume, chap. C; Horton and others, this volume, chap. A, chap. B). The structure lies beneath a seaward-dipping and seaward-thickening wedge of postimpact, middle to upper Cenozoic sediments. The postimpact section is about 250 m (820 ft) thick on the lower York-James Peninsula (Powars and Bruce, 1999; Gohn and others, this volume, chap. C) and thickens eastward to at least 396 m (1,300 ft) at the southern tip of the Delmarva Peninsula (Powars and Bruce, 1999).

The average diameter of the Chesapeake Bay impact structure, as illustrated by Poag (1997), Poag and others (1999), and Powars and Bruce (1999), is about 85 km (53 mi). The outer margin bounds an approximately 25-km-wide (15.5-mi-wide) annular trough that surrounds the structure's 35-km-wide (22-mi-wide), complexly deformed central crater. The seismic profile discussed in this chapter is located within the southwestern part of the annular trough of the Chesapeake Bay impact structure and is referred to as the "Langley seismic profile" (or survey).

Seismic Survey

Data Acquisition

The Langley seismic survey was conducted entirely on the premises of the NASA Langley Research Center at Hampton, Va., in September 2000. The Langley profile is 1,000 m (3,281 ft) long and trends approximately northeast to southwest (fig. I2). Acquisition parameters are shown in table I1.

Seismic sources were generated by a combination of explosions and seisgun blanks. We used the larger explosive sources to ensure propagation of seismic energy in the urban Hampton-Newport News area. Explosions were generated by 0.11-kilogram (0.25-pound) charges of ammonium nitrate at depths of approximately 3 m (10 ft). The explosions were spaced approximately every 25 m (82 ft) along the seismic profile, except near cultural features. Most seismic sources were generated by 400-grain, 8-gauge Betsy Seisgun blanks at depths of about 0.3 m (1 ft). The seisgun sources were spaced every 5 m (16.4 ft); however, seisgun sources were not generated at the locations of explosion shots. Thus, the effective spacing for seismic sources (explosions and blanks combined) was 5 m (16.4 ft) along the seismic profile.

Shot timing for the 0.11-kilogram (0.25-pound) explosions was determined by synchronized master clocks that are accurate to approximately 1 millisecond (ms). The master clocks controlled both the shot timing and the turn-on times for the seismographs. Shot timing for the Betsy Seisgun sources was determined electronically at the seismic source when the hammer electronically closed contact with the Betsy Seisgun, which also sent an electronic signal to the seismographs. Seismic sources were co-located (at 1-m (3.3-ft) lateral offset) with the geophones so that uphole times also were available for timing. To maintain a consistent start time, we removed 2 ms and 20 ms from the uphole times of explosive and seisgun sources, respectively. The consistent start time and calculated static corrections allowed data from both types of sources to be stacked together.

The seismic sources were recorded on an array of four Geometrics Strataview RX–60 seismographs, each with 60 channels. Along the Langley seismic profile, the setup of the seismic acquisition array allowed for 202 shots and 202 recording sites (geophones), which allows for a theoretical fold of 202 when the data are stacked. All 202 recording sites were utilized; however, because of cultural features (such as roadways and pipelines), 15 shotpoints were not utilized, and the resulting actual maximum fold was 187. We used 40-hertz (Hz), single-element, vertical-component Mark Products L–40A geophones to record the seismic signal. Approximately 5 seconds (s) of data were recorded for each shot at a sampling rate of 0.5 ms. The data were stored on the hard drive of the Geometrics Strataview RX–60 computers during field acquisition and were later downloaded to 4-millimeter (mm) tape for permanent storage in SEG-Y format (Barry and others, 1975).

Prior to acquiring the data, we measured distances between shotpoints with a meter tape and prepared shotholes at those locations. Individual recording sites also were predetermined and flagged to obtain the proper spacing. After the data were acquired, we used a high-precision differential Global Positioning System to measure the recording sites and shotpoint locations to accuracies of approximately 0.01 m (0.03 ft).

Data Processing

The long offset (about 1,000 m (3,281 ft) maximum) and multiple sources permitted both reflection and refraction data to be simultaneously acquired. We used two types of seismic data processing—seismic-refraction tomographic inversion and reflection-image processing. In refraction-data processing, we used the tomographic inversion method developed by Hole (1992), whereby first arrivals on each seismic trace were modeled to obtain detailed velocities along the profile.

Table I1. Acquisition parameters for the Langley seismic profile, Hampton, Va.

[ft, feet; Hz, hertz; kg, kilograms; lb, pounds; m, meters; ms, milliseconds; s, seconds]

Parameter	Description
Profile length	1,000 m (3,281 ft)
Timing	Electronic
Seismic sources	
Overall shot spacing	5 m (16.4 ft)
Explosion spacing	25 m (82 ft)
Explosion depth	3 m (10 ft)
Explosion type	0.11-kg (0.25-lb) charge of ammonium nitrate
Seisgun spacing	5 m (16.4 ft)
Seisgun depth	0.3 m (1 ft)
Seisgun type	400-grain, 8-gauge Betsy Seisgun
Seismic recording data	
Geophone spacing	5 m (16.4 ft)
Geophone type	40-Hz, single-element, vertical-component Mark Products L–40A geophone
Recording system	Array of 4 Geometrics Strataview RX–60 seismographs, each with 60 channels
Number of active channels	202
Sample rate	0.5 ms
Acquisition filters	None
Trace length	5 s

Table I2. Processing parameters for the Langley seismic profile, Hampton, Va.

[ft, feet; Hz, hertz; m, meters; m/s; meters per second; ms, milliseconds]

Parameter	Description
Maximum fold	187
Common-depth-point spacing	2.5 m (8.2 ft)
Deconvolution	21 ms/200 ms
Automatic gain control (AGC)	
Prestack	300 ms
Poststack	100 ms
Bandpass filtering	
Prestack	25–50–600–1,200 Hz
Poststack	30–60–600–1,200 Hz
Frequency-distance (F-K) filtering	
F-K acceptance level	>1,000 m/s
F-K rejection level	1–200 Hz
Migration	
Angle	25°
Aperture	400 m
Frequency	400 Hz

Approximately 40,000 first arrivals were used to develop the velocity model, and all first-arrival measurements were checked for reciprocity between shot and receiver pairs. However, lower velocity sediments underlying higher velocity sediments at depths of about 50 m (164 ft) limited measurement of refraction velocities to the upper 50 m (164 ft). From about 50 m (164 ft) to about 635 m (2,083.3 ft), velocities were determined from the sonic velocity (interval transit time) log measured within the USGS-NASA Langley corehole located near the center of the seismic profile. The models are described in the next section.

Seismic-reflection data were processed by generally following the procedure outlined by Brouwer and Helbig (1998). Parameters used in processing are shown in table I2. Processing steps included the following: geometry installation, independent trace editing (to remove noisy traces or data from malfunctioning geophones), timing corrections, elevation static corrections, automatic-gain-control (AGC) bandpass filtering, frequency-distance (F-K) filtering, velocity analysis (from refractions and sonic log), normal-move-out correction, stretch muting, common-depth-point (CDP) stacking, Kirchoff prestack depth migration, poststack AGC, poststack bandpass filtering, poststack deconvolution, and time-to-depth conversion (for unmigrated data).

Seismic Data and P-Wave Velocity Models

All shots, whether seisgun or explosive, propagated the entire length of the recording array. A typical explosive shot record is shown in figure I4. Numerous clear reflections are observed from about 0 ms to about 700 ms, and first-arrival refractions are observed along the length of the Langley profile.

Compressional wave (P-wave) velocities in the upper 50 m (164 ft) range from about 800 meters per second (m/s; 2,625 feet per second (ft/s)) to about 1,700 m/s (5,577 ft/s) and are laterally continuous with minor variations (fig. I5*A*). A relatively low velocity gradient is apparent below about 50 m (164 ft) depth (fig. I5*B*).

Corehole sonic velocities were calculated from acoustic interval-transit times acquired approximately every 3 centimeters (0.1 ft) in the Langley corehole by the interval-transit-time

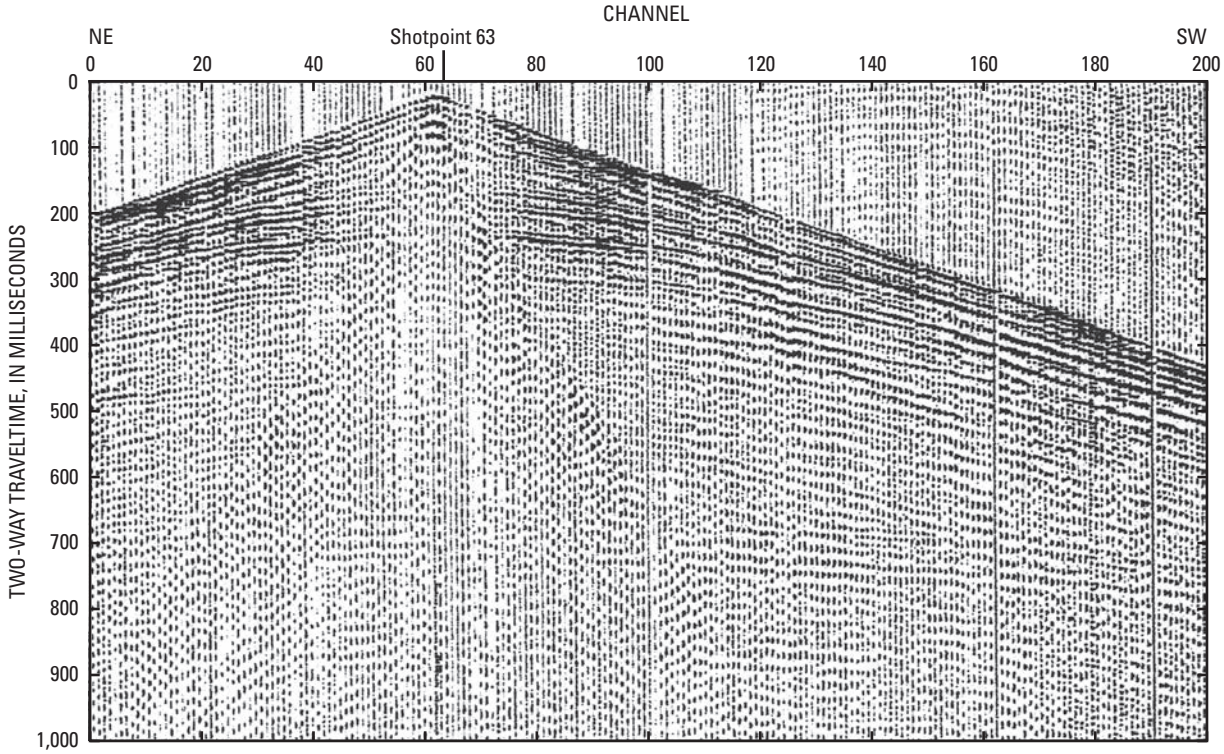

Figure I4. Explosion shot gather at shotpoint 63 from the Langley seismic profile showing the reflective nature of the subsurface from the surface to about 700 ms and the clear first-arrival refractions. A channel was located at each shotpoint.

sonde (fig. I5*B*). Appreciable scatter in the data suggests a range of velocities at all depths and (or) measurement errors that likely resulted in part from "cycle skipping" produced by excessive signal attenuation. We selected representative velocities within the range of scatter as shown in figure I5*B*.

In general, the sonic measurements suggest that velocities are relatively low (less than 2,500 m/s, or 8,202 ft/s) for most of the subsurface above basement. The data show a high-velocity cap at about 50 to 62 m (164 to 203 ft) depth, where velocities range from about 2,500 m/s (8,202 ft/s) to about 3,000 m/s (9,843 ft/s). From about 60 m (197 ft) to about 140 m (459 ft) depth, average velocities range between about 1,500 m/s (4,921 ft/s) and about 2,000 m/s (6,562 ft/s), and the overall trend is toward a slight negative gradient. This lower velocity or the negative gradient limits the surface-based refraction measurements. From about 140 m (459 ft) to about 180 m (591 ft) depth and from about 235 m (771 ft) to 275 m (902 ft) depth, relatively higher velocities also are observed (about 2,000 to 2,200 m/s, or 6,562 to 7,218 ft/s), but these velocities are generally lower than those at 60 m (197 ft) depth. The relatively low velocities between about 60 m (197 ft) depth and crystalline basement near 625 m (2,051 ft) depth prevent surface-based refracted energy from returning to the surface. In crustal-scale refraction seismology, lower velocity materials that underlie higher velocity materials are commonly referred to as low-velocity zones, shadow zones, or velocity inversions.

Seismic-Reflection Images

We stacked shot gathers along the Langley profile to produce seismic-reflection images of the upper 1,000 m (3,281 ft) of section. Common-depth-point (CDP) traces are located every 2.5 m (8.2 ft) along the seismic profile. Time-distance, unmigrated depth-distance, and migrated depth-distance plots were generated (figs. I6, I7, and I8). Depths were calculated by assuming the velocity profile shown in figure I5. The data are plotted as positive polarity.

Vertical resolution of the seismic images depends on the velocities and frequencies used to generate the images. Velocities generally range from about 800 m/s (2,625 ft/s) to about 3,000 m/s (9,843 ft/s) in the upper 600 m (1,969 ft), and frequencies range from about 30 to 600 Hz. When the one-quarter wavelength criteria (Waters, 1981) are used, the minimum thickness of imaged reflectors ranges between about 1 m (3.3 ft) and 15 m (49.2 ft).

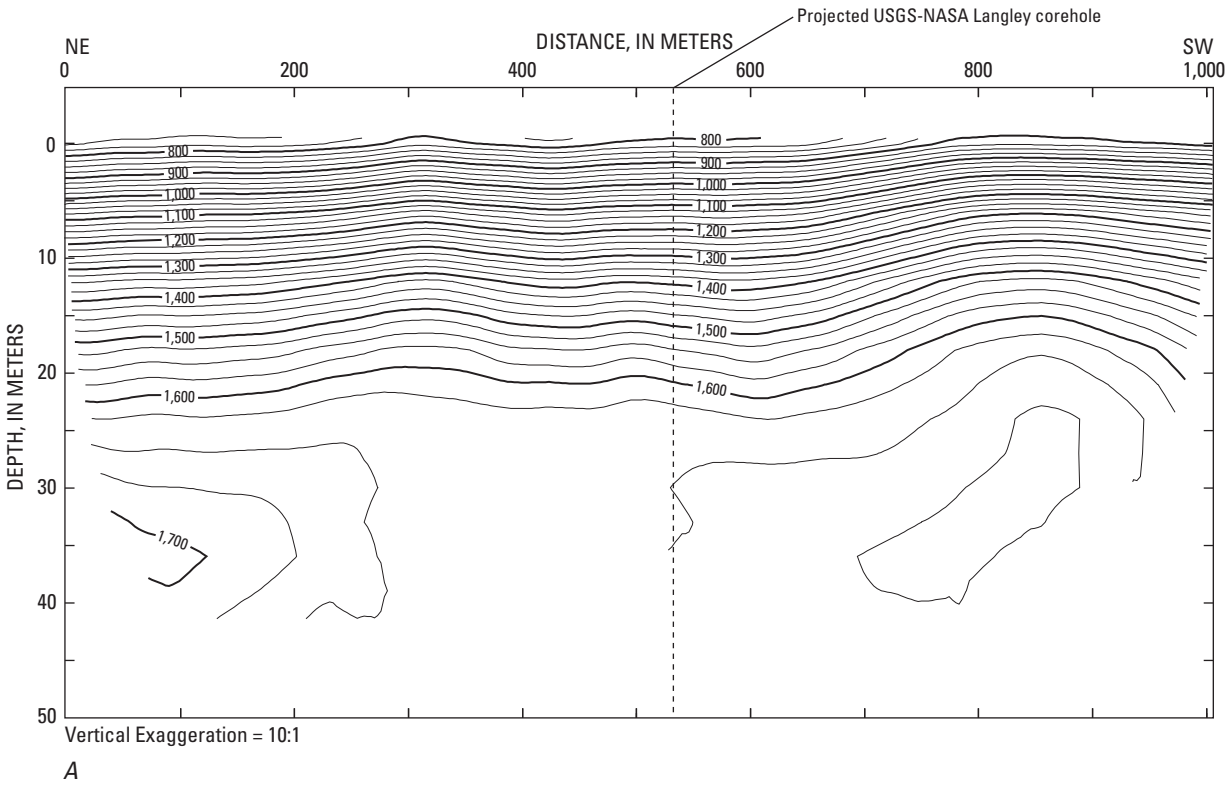

Figure I5. Velocity model from the Langley seismic profile and velocity log from the USGS-NASA Langley corehole. *A,* Two-dimensional velocity model along the Langley profile derived from inversion of first-arrival refractions. Contours show P-wave velocities in meters per second. *B,* One-dimensional velocity model (solid line) derived from the sonic velocity (interval transit time) log collected in the Langley corehole. The left track displays every second data point in the corehole dataset. The right track displays every tenth data point in the dataset. The stratigraphy of the corehole section is shown on the left: Ple, Pleistocene; DC, Drummonds Corner beds; NP, Neoproterozoic; LG, Langley Granite.

The three seismic images show numerous reflections across their full depth of 1,000 m (3,281 ft). Reflections above 635.1 m (2,083.8 ft) depth are correlated with the geologic units identified in the USGS-NASA Langley core (Gohn and others, this volume, chap. C; Poag and Norris, this volume, chap. F; Powars and others, this volume, chap. G).

Time-distance image.—Numerous reflections are observed along the Langley profile from about 25 ms to about 740 ms (fig. I6). Although the entire section is reflective above 740 ms, the nature of the reflections varies appreciably within differing time intervals. Laterally continuous reflections are particularly pronounced from about 25 ms to 50 ms and from about 200 ms to about 400 ms. However, reflections between about 400 ms and about 670 ms are largely laterally discontinuous, except for several clear southwest-dipping reflections on the northeastern half of the profile and less obvious northeast-dipping reflections on the southwestern half of the profile. The fewest laterally coherent reflections occur from about 740 ms to about 1,000 ms.

Most reflections above 670 ms indicate slight vertical displacement along the profile, and small diffractions are apparent on the section. An apparent vertical offset in reflections at 700 ms (meter 550 of the profile) also shows diffracted energy originating at the location of the offset. Such diffractions usually can be attributed to lateral velocity variations caused by faulting and fracturing that result in abrupt truncations of layers (Anstey, 1977).

Unmigrated depth-distance image.—We converted the time-distance seismic image (fig. I6) to an unmigrated depth-distance seismic image (fig. I7) by using the combined refraction and sonic velocity model (fig. I5). In stacking, velocities in the upper 50 m (164 ft) varied laterally as determined by the refraction velocity model, but we used laterally constant velocities from the sonic log below 50 m (164 ft) depth. The depth-distance image shows laterally continuous reflections in the depth ranges from about 0 m to 50 m (about 0 ft to 164 ft), 150 m to 325 m (about 492 ft to 1,066 ft), and 625 m to 800 m (about 2,051 ft to 2,625 ft). From about 325 m to about 625 m (about 1,066 ft to about 2,051 ft) depth, the subsurface is less reflective, and reflections are laterally discontinuous. Southwesterly and northeasterly dipping reflections also are apparent, as observed in the time section (fig. I6). Reflections below about 625 m (2,051 ft) appear much thicker and higher in amplitude than those higher

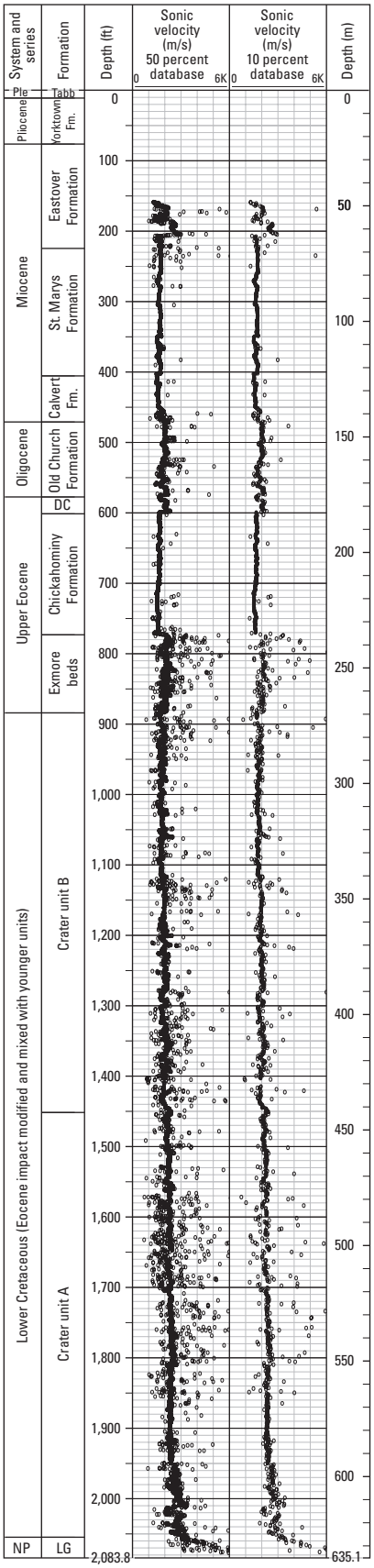

B

Figure I5. Continued.

in the section. Slight vertical offsets are apparent, as observed on the time section, and these offsets correlate with diffracted energy, suggestive of faulting and fracturing.

Migrated depth-distance image.—We used Kirchoff prestack depth migration to collapse the diffracted energy observed on the time and depth sections. The resulting migrated depth-distance section (fig. I8) shows much the same reflectivity pattern as the unmigrated depth section (fig. I7); however, numerous small offsets in reflectors are apparent where the diffracted energy was collapsed. Although there are some small offsets in layers above about 325 m (1,066 ft) depth and at 625 m (2,051 ft) depth, a far greater number of small offsets (faults or fractures) are observed from about 325 m to about 625 m (about 1,066 ft to about 2,051 ft) depth. Migration also shows that the dipping reflections between 325 m and 625 m (1,066 ft to 2,051 ft) depth merge into subhorizontal reflections near the northeastern and southwestern ends of the profile. Migration allows a more accurate placement of the top of basement.

Geologic Interpretation of Seismic Images

Coastal Plain Basement

We interpret the top of basement rocks as the nearly continuous, wavy, high-amplitude reflection that varies in depth between 630 m and 625 m (2,067 ft and 2,051 ft) on the migrated depth image (figs. I9, I10, and I11). These depths are in good agreement with the top of weathered granite found at 626.3 m (2,054.7 ft) depth in the Langley core (fig. I3); this granite is named the Langley Granite by Horton and others (this volume, chap. B). Granite was recovered to the bottom of the Langley corehole at a depth of 635.1 m (2,083.8 ft). This cored section consists of variably weathered, pale-red, medium-grained, homogeneous granite of Neoproterozoic age (Horton and others, this volume, chap. B).

The time-distance and depth-distance sections (figs. I6 and I7) show at least three major reflections at and below the top of the granite. We interpret the shallowest reflection as the sediment-weathered rock contact, the second reflection as the weathered rock-to-unweathered rock transition, and the third reflection as a reverberation arising from the weathered and unweathered contacts. These reflections are widely spaced on the unmigrated and migrated depth sections because of the high basement velocities used to convert from time to depth. This interpretation suggests that the weathered rock is about 40 m (131 ft) thick. The recovered 8.9-m-long (29.1-ft-long) granite core is strongly weathered and crumbly in its upper part but grades down to partially weathered, hard granite in the basal 0.9 m (3 ft) of the core (Horton and others, this volume, chap. B). Weathering along mineral veins and mineralized fractures and faults observed in the core (Horton and others, this volume, chap. B) may be a contributing factor to the large thickness of the weathering zone inferred from the seismic images.

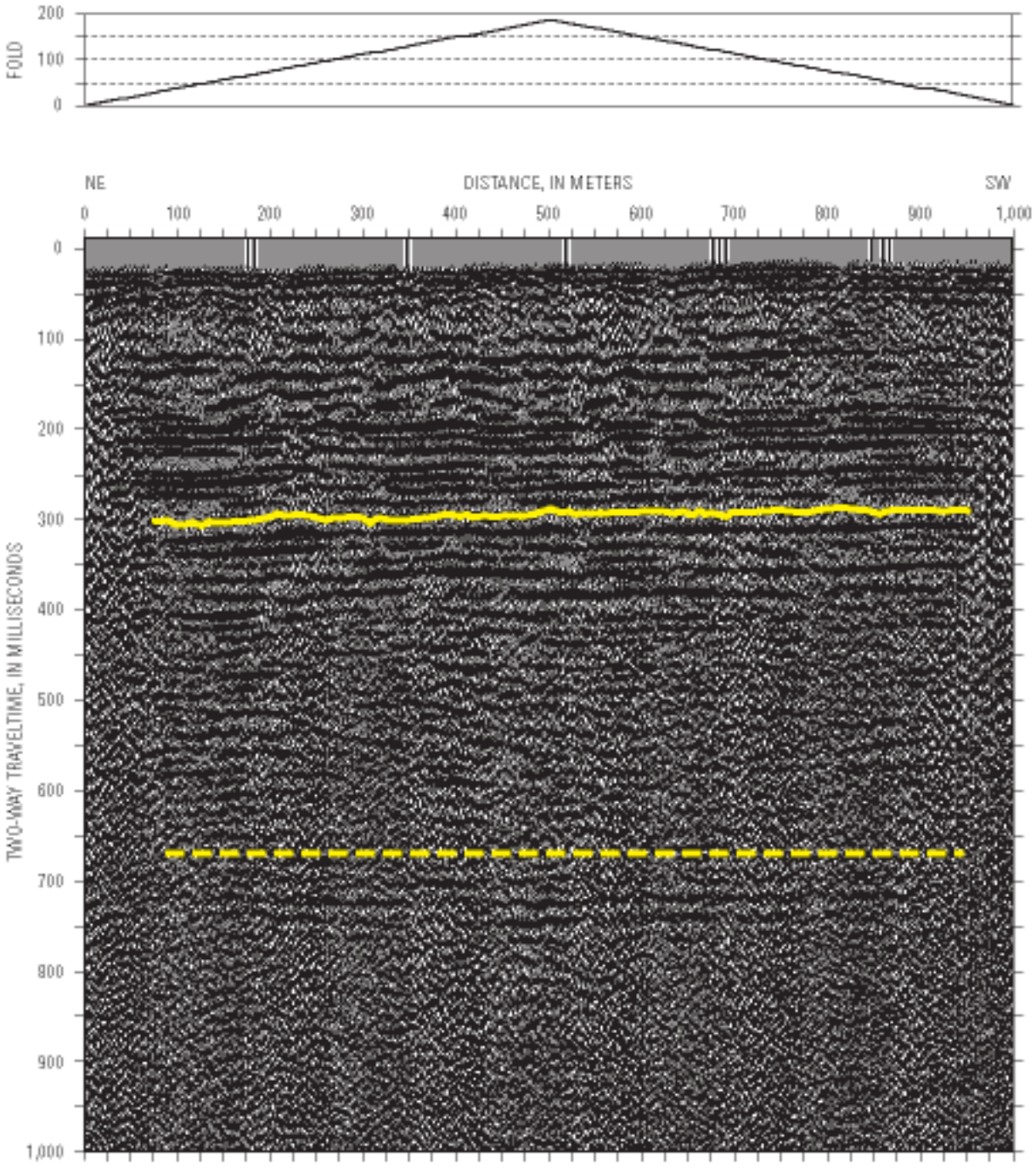

Figure I6. Time-distance seismic-reflection image for the Langley profile. The lower highlighted boundary (at about 670 ms) is between crystalline basement rocks (the Langley Granite in the USGS-NASA Langley core) and overlying preimpact sediments. The upper highlighted boundary (at about 300 ms) is between preimpact and synimpact sediments and overlying postimpact sediments. The seismic sources were energetic enough to provide signals from depths of about 1 km (0.6 mi) along part of the seismic profile with a fold of only 1.

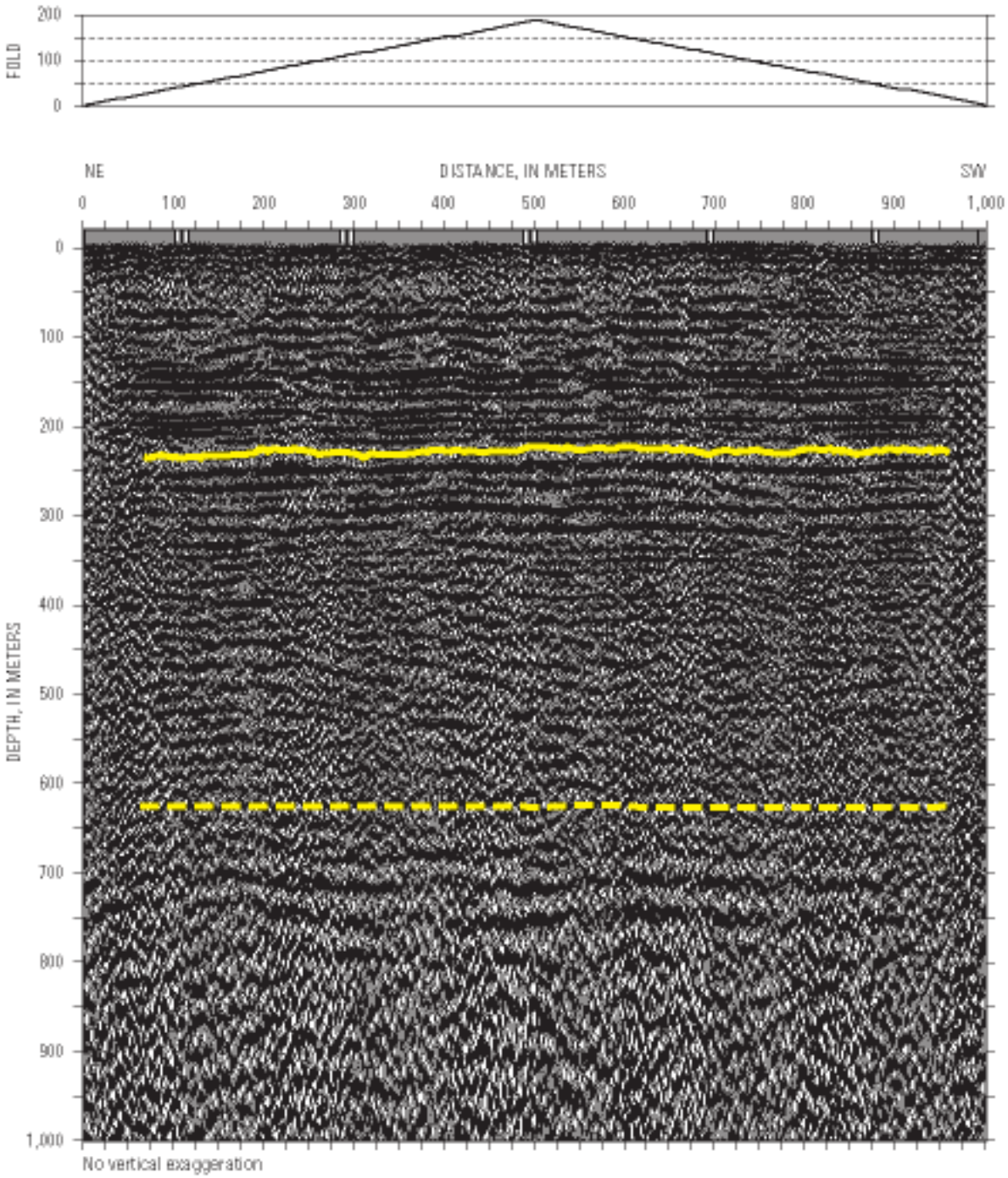

Figure I7. Unmigrated depth-distance seismic-reflection image for the Langley profile. The lower highlighted boundary (at about 625 m, 2,051 ft) is between crystalline basement rocks (the Langley Granite in the USGS-NASA Langley core) and overlying preimpact sediments. The upper highlighted boundary (at about 240 m, 787.4 ft) is between preimpact and synimpact sediments and overlying postimpact sediments.

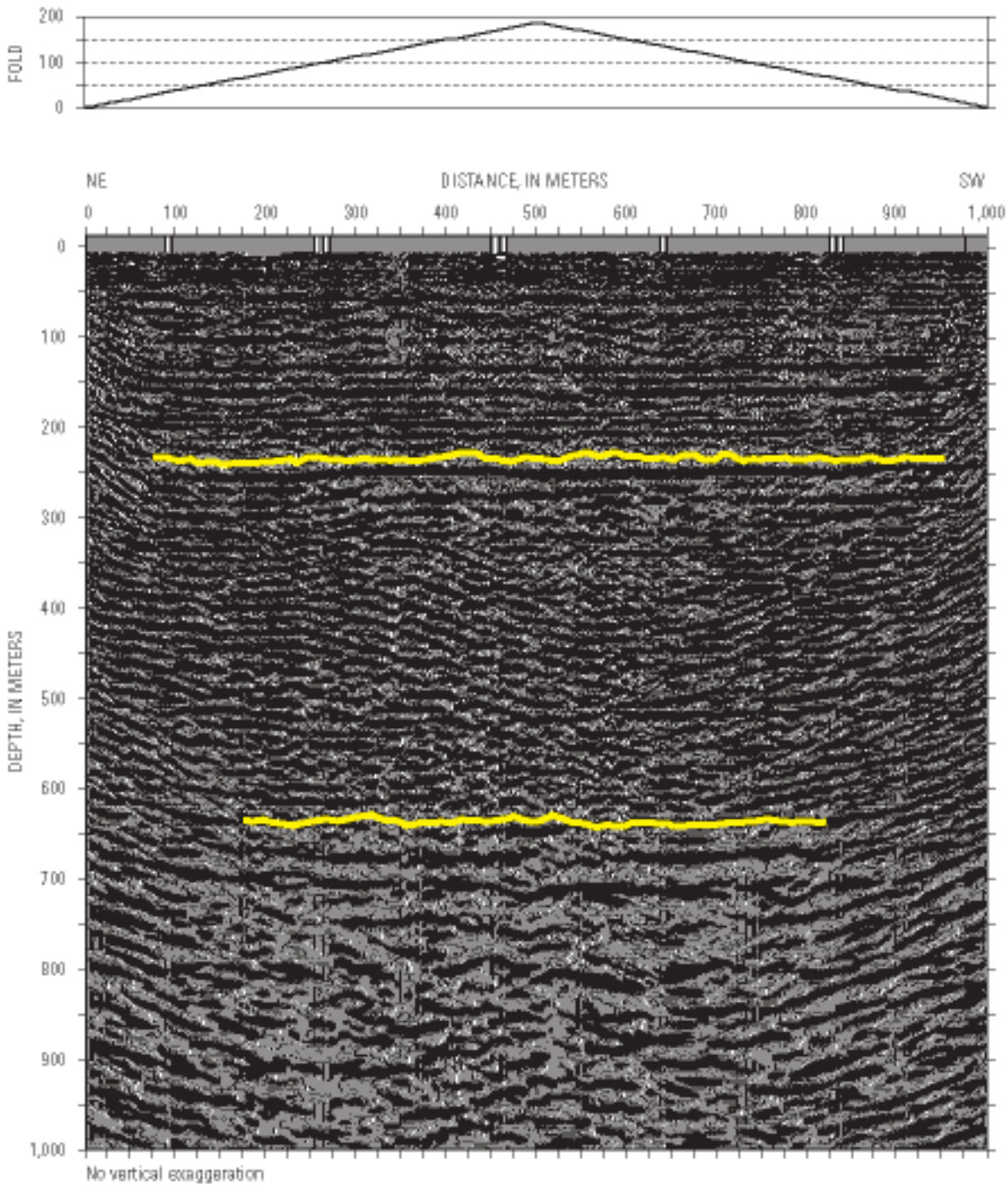

Figure I8. Migrated depth-distance seismic-reflection image for the Langley profile. Highlighted boundaries as in figure I7. Migration allows a more accurate placement of the top of basement than in the unmigrated section.

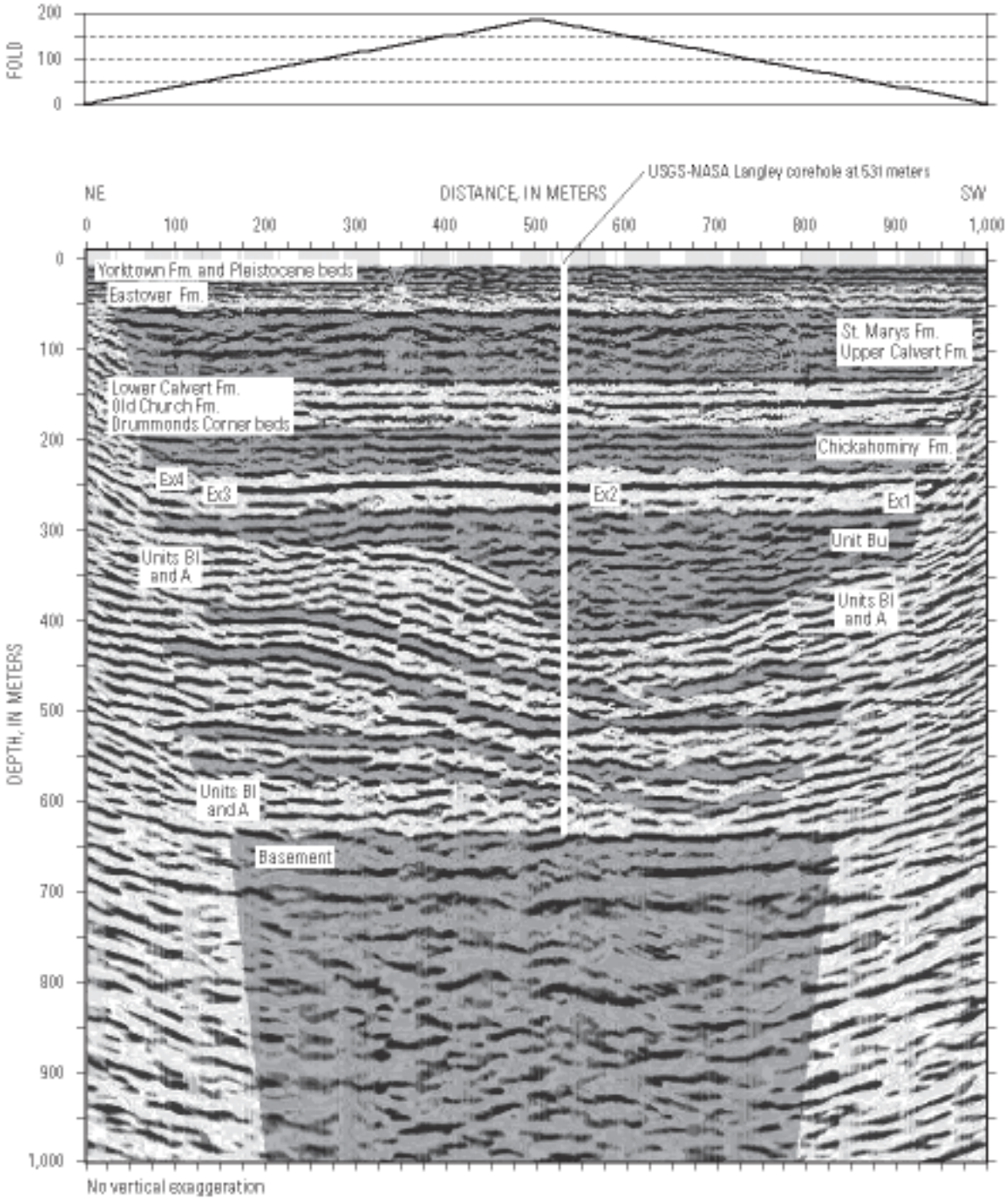

Figure I9. Interpreted migrated depth image for the Langley profile showing the major impact-related and postimpact seismic-stratigraphic units discussed in the text. Unit designations: A, crater unit A; Bl, lower beds of crater unit B; Bu, upper beds of crater unit B; Ex1, Ex2, Ex3, and Ex4, seismically defined subunits of the Exmore beds; Fm., formation.

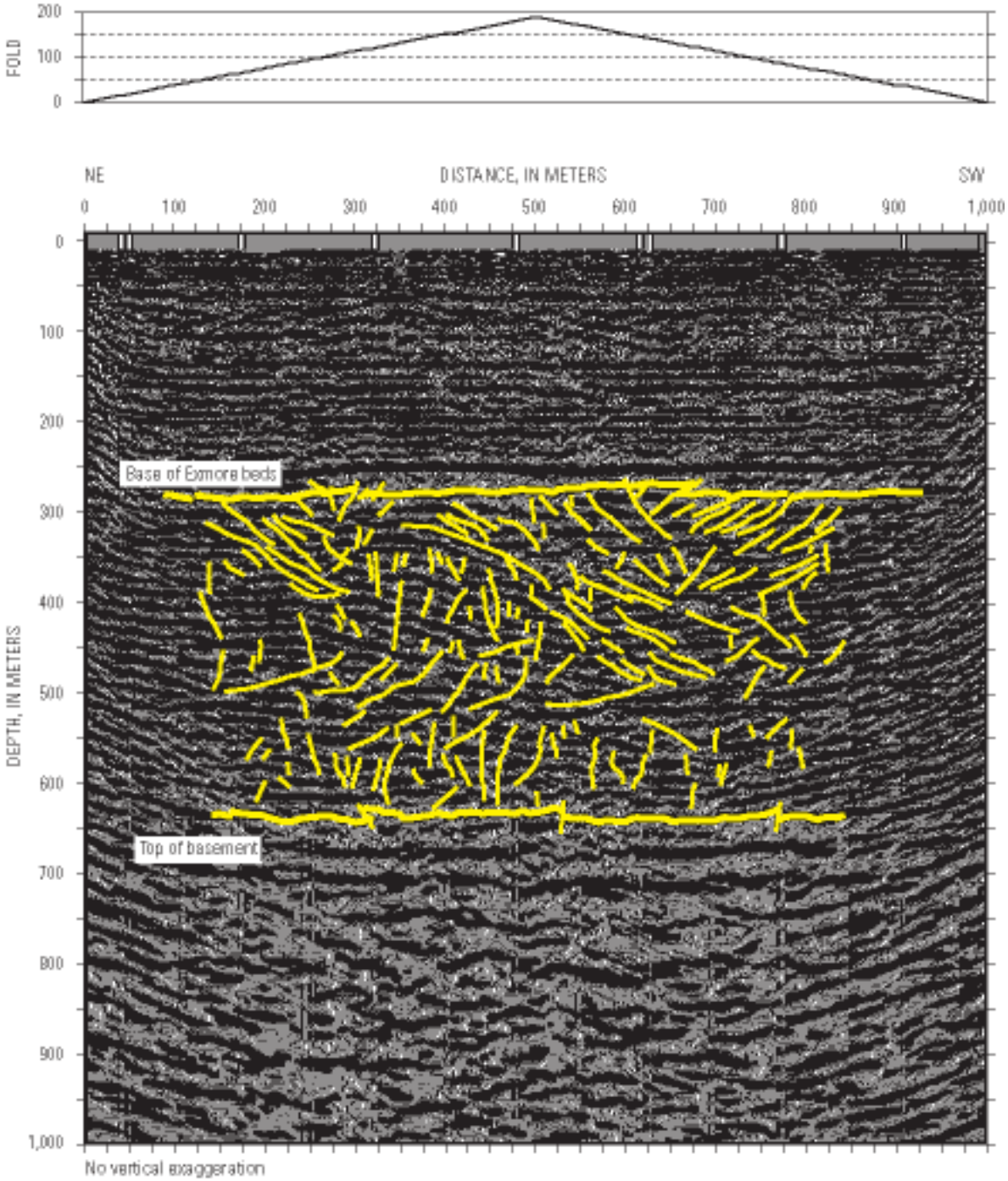

Figure I10. Interpreted migrated depth image for the Langley profile showing the distribution of small-offset faults (short yellow lines) in crater units A and B between highlighted boundaries representing the top of basement rocks and the base of the Exmore beds.

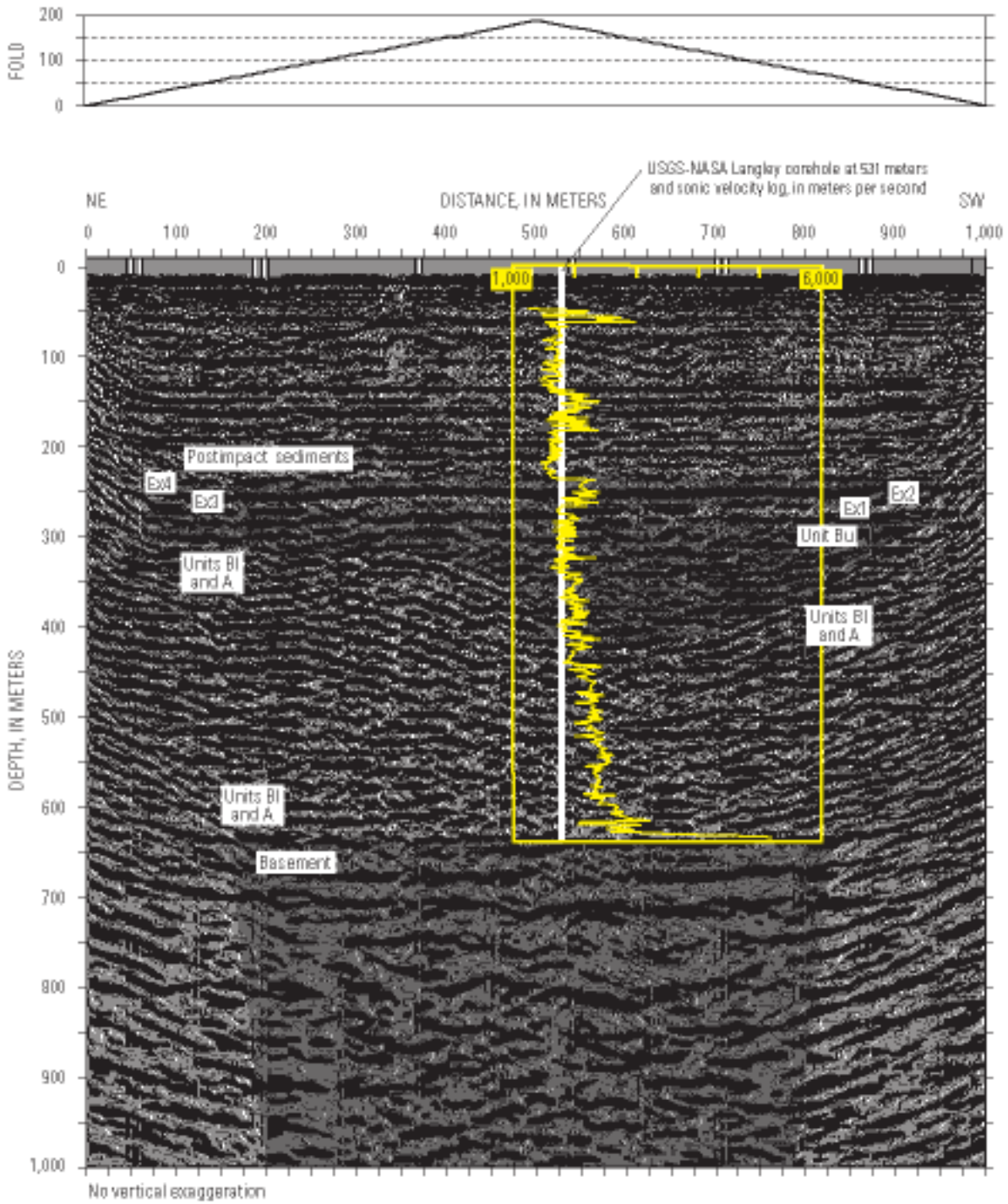

Figure I11. Interpreted migrated depth image for the Langley profile showing the seismic-stratigraphic units and generalized sonic velocity data acquired in the USGS-NASA Langley corehole (fig. I5*B*). Sonic velocities range from about 1,500 to about 5,500 meters per second (m/s). Note that the seismically defined subunits of the Exmore beds (Ex1, Ex2, Ex3, and Ex4) are variably shaded.

Horizontal, discontinuous, wavy, high-amplitude reflections characterize most of the basement section on the migrated depth image (fig. I9). Diffractions on the time-distance and depth-distance images (figs. I6 and I7) suggest that the basement section contains numerous inhomogeneities. In addition, inferred high-angle faults of uncertain extent displace the top of basement by less than 10 m (33 ft) at several places on the migrated depth image (fig. I10).

The granite core from the Langley corehole is too short to address the source of the horizontal, wavy reflections. However, the common mineral veins and mineralized fractures and faults in the core dip at all angles from vertical to horizontal and could be the source of the diffractions seen on the unmigrated images (Horton and others, this volume, chap. B). The granite is assumed to extend significantly below the base of the rocks depicted in the seismic images.

Impact-Modified Sediments

Core Stratigraphy

The impact-modified sedimentary section in the Langley core primarily consists of Lower Cretaceous and basal Upper Cretaeous fluvial sediments of the Potomac Formation. This variably deformed section is divided informally into crater unit A and overlying crater unit B (Frederiksen and others, this volume, chap. D; Gohn and others, this volume, chap. C). The unit contact is placed at the base of the lowest occurrence of injected exotic glauconitic sediments at 442.5 m (1,451.7 ft) depth (fig. I3). The contact between crater unit B and the overlying Exmore beds is placed at a depth of 269.4 m (884.0 ft). Reflections within crater units A and B (figs. I6, I7, I8, I9, and I10) are interpreted to represent primary bedding within the Potomac Formation.

Crater unit A is divided into two subunits in the Langley core—the lower beds and the upper beds (Gohn and others, this volume, chap. C). The subunit contact is placed at a depth of 558.1 m (1,831.0 ft) (fig. I3). The lower beds consist of nearly pristine sands, silts, and clays of the Potomac Formation, in which primary horizontal stratification is well preserved, clay-silt beds are only moderately fractured, and primary sedimentary structures and cycles typical of the Potomac Formation outside the impact structure are intact. In the upper beds, however, zones of structureless fluidized sand up to 17 m (55.8 ft) thick and strongly fractured clay-silt layers are present locally. Crater unit A does not contain igneous-rock or sediment ejecta, shocked quartz grains, or exotic preimpact Tertiary sediments (Gohn and others, this volume, chap. C; Horton and Izett, this volume, chap. E).

Crater unit B also is divided informally into lower beds and upper beds; the contact is at 427.7 m (1,403.3 ft) depth (fig. I3). The lower beds consist of locally fluidized and fractured sediments of the Potomac Formation similar to those found in the upper beds of crater unit A. Exotic injected glauconitic sediments are present only in a 0.3-m-thick (1.0-ft-thick) zone at the base of the lower beds of crater unit B (fig. I3).

The upper beds of crater unit B in the core consist of megablocks (1 m to 25 m (3.3 ft to 82.0 ft) in diameter) and megablock zones (intervals of multiple megablocks with block-on-block contacts) of fragmented sediments of the Potomac Formation (Gohn and others, this volume, chap. C). Fractures and steeply dipping primary stratification are common within the megablocks and indicate postdepositional movement and rotation.

The megablocks and megablock zones are separated by intervals consisting of blocks of sediment of the Potomac Formation (4 mm to 1 m (0.16 inch to 3.3 ft) in diameter) suspended in a muddy, sandy, and gravelly matrix of native disaggregated sediments of the Potomac Formation and downward-injected, exotic, disaggregated, glauconitic Upper Cretaceous and Tertiary marine sediments. Gohn and others (this volume, chap. C) refer to these lithologically heterogeneous intervals as matrix zones. The presence of exotic Upper Cretaceous and Tertiary marine sediments is inferred from the large amount of glauconite sand in the matrix zones; glauconite is very sparse in the Potomac Formation but is very common in the preimpact Upper Cretaceous and Tertiary sections (Powars and Bruce, 1999; Gohn and others, this volume, chap. C). Shocked quartz has not been found in the upper beds of crater unit B, except in one piece of igneous-rock ejecta found near the top of the unit, and exotic lithoclasts of preimpact Upper Cretaceous and Tertiary marine sediments are absent (Gohn and others, this volume, chap. C; Horton and Izett, this volume, chap. E).

Seismic Images

Semicontinuous, horizontal and moderately dipping reflections between depths of about 625 m (2,051 ft) and about 420 m (1,378 ft) near the corehole represent crater unit A and the lower beds of crater unit B (unit Bl) of the Langley core (figs. I3 and I9). Thicker combined sections of these units are present northeast and southwest of the corehole.

Horizontal reflections in crater units A and Bl near the northeastern end of the profile dip to the southwest at moderate apparent angles beginning between meters 250 and 300 of the distance scale and continuing past meter 500 to the vicinity of the corehole, where their dip angles generally flatten (fig. I9). Similarly, subhorizontal reflections in crater units A and Bl near the southwestern end of the profile dip to the northeast at moderate apparent angles beginning near meters 750 to 800 of the seismic profile (distance scale) and continuing to near the corehole, where their dip angles also decrease. (The outermost zones of unusually steep dips on figure I9 are artifacts of the migration process.) Within the interval of dipping reflections, apparent dip angles tend to decrease downsection from about 25° in the upper part of the interval to less than 10° near the base of the interval. Structural relief on the order of 75 m (246 ft) is apparent for some dipping reflections in the northeastern part of the structure. Four pairs of high-amplitude reflections in combined units A and Bl are shaded in figure I9 to illustrate the unit's internal structure.

The upper contact of combined crater units A and Bl mimics their internal structure (fig. I9). This contact is near a depth of 300 m (984 ft) at the northeastern end of the profile but dips downward, and cuts stratigraphically downsection, to a depth of about 420 m (1,378 ft) near the corehole. From there, the contact is interpreted to rise in elevation to the southwest. The position of the top of combined crater units A and Bl is not readily determined southwest of meter 800 (distance scale) on the migrated depth image; the position of this contact in this area is drawn provisionally in figure I9. Approximately 120 m (394 ft) of relief are present along this surface. In contrast, the lower contact of crater unit A with the basement granite is horizontal and has only minor relief.

Vertical to moderately dipping faults that have short lengths (tens of meters) and small displacements on the order of a few meters to 10 m (33 ft) are apparent throughout combined crater units A and Bl on the migrated depth image. The complexity of the faulting does not permit a unique interpretation of fault locations and displacements; our interpretation is shown in figure I10. Individual faults typically offset one to four reflections. The lateral spacing of these faults is irregular but may be as small as about 10 m (33 ft). Normal and reverse faults are present in this fault population, and similar faults having smaller displacements below the resolution of the seismic image also may be present.

In our interpretation (fig. I10), there is a change in fault dip angles at or near the contact between the lower beds and the upper beds of crater unit A, which is placed at 558.1 m (1,831.0 ft) depth in the Langley core. Fault dip angles above this depth typically are moderate, although some steeply dipping faults also are present; below this depth, steeply dipping faults predominate. Faults in crater units A and B of the Langley core include vertical to moderately dipping dip-slip faults and a few horizontal faults (Gohn and others, this volume, chap. C; Horton and others, this volume, chap. B).

The upper beds of crater unit B (unit Bu) are represented by a planar-convex interval of discontinuous and locally weak, isolated, and (or) inclined reflections on the migrated depth image (fig. I9). There is a general trend toward greater continuity of individual reflections within crater unit Bu from the center to the ends of the seismic profile. The small-offset faults seen in crater units A and Bl also are observed in crater unit Bu (fig. I10).

The high-relief contact between combined crater units A and Bl and overlying crater unit Bu is defined on the migrated depth image by angular relationships and offsets between reflections, except near meter 600 of the profile southwest of the Langley corehole where the reflections appear conformable or paraconformable (fig. I9). The truncation and offset of reflections at the contact suggest that it locally consists of low- to moderate-angle dip-slip faults.

Impact-Generated Sediments

Variations of the informal name “Exmore beds” have been applied to the impact-generated polymict sedimentary breccias that underlie the postimpact, upper Eocene Chickahominy Formation and typically cap the impactite section of the Chesapeake Bay impact structure (Powars and others, 1992; Poag, 1997; Powars and Bruce, 1999). We place the lower and upper contacts of the Exmore beds at approximately 270 m (886 ft) and 235 m (771 ft) depths, respectively, in the center of the migrated depth section (fig. I9), in agreement with the contacts of the Exmore beds in the Langley core at depths of 269.4 m (884.0 ft) and 235.65 m (773.12 ft) (Gohn and others, this volume, chap. C).

In the Langley core, the Exmore beds consist of pebbles, cobbles, and boulders (typically smaller than 1 m (3.3 ft) in diameter) suspended in an unsorted and unstratified matrix of calcareous, muddy, very fine to very coarse sand and granules. The clasts primarily consist of sediment lithoclasts derived from the preimpact Cretaceous and lower Tertiary formations of the area (Powars and Bruce, 1999; Gohn and others, this volume, chap. C). The sand fraction of the matrix consists primarily of quartz and glauconite. Shocked and (or) cataclastic igneous-rock lithoclasts also are present, and shocked quartz grains are present but sparse in the Exmore matrix (Horton and Izett, this volume, chap. E).

We interpret the Exmore beds to consist of four subunits on the migrated depth profile (figs. I9 and I11). Exmore subunits 1, 2, and 3 are bounded by inclined, overlapping reflections that progressively overstep the underlying reflection from southwest to northeast toward the crater’s center. Therefore, the base of the Exmore beds is a composite surface within the limits of the Langley profile as a result of the overstepping contacts. The base of Exmore subunit 4 is the high-amplitude reflection near 250 m (820 ft) depth, along which subunit 4 overlies subunits 2 and 3. The upper contact of the Exmore beds with the overlying fine-grained sediments of the Chickahominy Formation is a wavy, semicontinuous reflection.

Postimpact Sediments

A provisional analysis of the distribution of individual and composite postimpact stratigraphic units on the migrated depth image is illustrated in figure I9. The postimpact section extends from the top of the Exmore beds at about 235 m (771 ft) depth to the top of the image. The corresponding section in the Langley core consists of 235.65 m (773.12 ft) of upper Eocene through Pliocene marine sediments and Pleistocene paralic deposits (Edwards and others, this volume, chap. H; Powars and others, this volume, chap. G).

The postimpact units are characterized by horizontal, semicontinuous and continuous reflections at their boundaries and internally. Fine-grained shelf deposits of the upper Eocene Chickahominy Formation above the Exmore beds are overlain by a composite section of glauconitic or shelly sediments of the

Oligocene Drummonds Corner beds and Old Church Formation and the lower Miocene part of the Calvert Formation (fig. I9). That section is overlain by a composite section of middle Miocene siliceous clay-silts of the upper part of the Calvert Formation and overlying upper Miocene calcareous clay-silts of the St. Marys Formation. Shelly, clayey silts and muddy fine sands of the upper Miocene Eastover Formation overlie the St. Marys. Above the Eastover, a composite unit consisting of shelly, muddy fine sands of the Pliocene Yorktown Formation and thin, sandy, estuarine(?) Pleistocene sediments completes the postimpact section.

Wavy reflections within specific stratigraphic intervals in the postimpact section may result from lateral velocity variations produced by lateral lithologic changes. These wavy reflections are best developed in the undifferentiated upper Calvert-St. Marys section.

Discussion

Collapse Structure

We interpret the major structural feature observed on the Langley seismic images (figs. I6, I7, I8, I9, I10, and I11) as a stratabound, extensional collapse structure. This structure is defined on the seismic images by the dipping (downward-displaced), truncated reflections in crater units A and B and in the Langley core by the style and intensity of sediment disruption in those units. The structure is confined vertically to the sedimentary section of the impact structure's annular trough. Deformation of this magnitude is not present along the low-angle, low-relief contact of crater unit B with the Exmore beds above the collapse structure nor below the structure along the subhorizontal, low-relief top of the granite or within the lower beds of crater unit A (fig. I9). The variable dip directions and variable and relatively steep apparent dip angles of bedding (reflections) within the collapse structure are not typical of the Atlantic Coastal Plain, where seaward dips of less than 1° are normal (Olsson and others, 1988).

The lateral boundaries of the collapse structure cannot be located precisely. Major normal faults apparently do not bound the collapsed section; instead, the displacements required by the structure are distributed among numerous small-displacement, subvertical faults (fig. I10), possible bedding-parallel faults, and fluidized sand layers. The structure is interpreted to be about 550 m (1,805 ft) in maximum width between meters 225 (738 ft) and 775 (2,543 ft) of the seismic profile (fig. I9).

We suggest that fluidized sand beds in crater unit A at 558 m (1,831 ft) depth and above (Gohn and others, this volume, chap. C) provided the necessary low-strength zone in the lower part of the collapsed interval. Upward loss of formation water from the fluidized sands through the pervasive network of small-offset faults (fig. I10), in combination with sand grain compaction, would have provided the accommodation space needed in the lower part of the collapse structure.

An inferred detachment zone near 558 m (1,831 ft) depth separates fluidized sands and fractured clays in the upper beds of crater unit A and in crater unit B from the lower beds of crater unit A and the underlying granite, in which no unequivocal evidence for impact deformation is observed in the Langley core (Gohn and others, this volume, chap. C; Horton and others, this volume, chap. B). The apparent dip angles of reflections in crater unit A also decrease significantly at this approximate depth (fig. I9), and the observed change in the predominant dip angles of the small-displacement faults also occurs at this depth (fig. I10).

The collapse structure described in this chapter may be analogous to fault-bounded grabens in the early Tertiary Silverpit impact structure of the North Sea, described by Stewart and Allen (2002). Stratabound grabens delimited by steep, facing normal faults are the major structures in the outermost zone (zone 3) of the Silverpit impact structure. Cretaceous sedimentary strata between the grabens appear relatively undeformed and horizontal, which is also the case for most of the strata seen on our seismic transect on the York-James Peninsula. The Silverpit grabens have widths (hundreds of meters) and vertical structural displacements (tens of meters) similar to those of the Langley collapse structure. Differences in lateral boundary structures between the normal-fault-bounded Silverpit grabens and the distributed structural displacements of the Langley collapse structure may result from differences in sediment compaction and lithification between Cretaceous chalks at Silverpit and Cretaceous sands and clays of the Potomac Formation at Langley.

Stewart and Allen (2002) suggested that overpressured chalk layers in a chalk-clay sequence provided detachment zones at depths equal to the lower terminations of the graben-bounding normal faults at Silverpit. They also suggested that fractures acted as dewatering conduits that produced the volume accommodation needed at the bottoms of the grabens.

In plan view, the Silverpit grabens and other normal faults define a concentric multi-ring structural pattern in the outer part of the 20-km-wide (12-mi-wide) Silverpit impact structure (Stewart and Allen, 2002). Powars and others (2003) have suggested the possibility of a similar concentric structural pattern in the Chesapeake Bay impact structure. Confirmation of the Chesapeake Bay crater-Silverpit crater analogy ultimately will require a three-dimensional grid of reflection profiles near Langley or elsewhere within the annular trough of the Chesapeake Bay impact structure.

The annular troughs of complex impact craters result from late-stage, gravity-driven collapse across an area that is significantly wider than the short-lived transient crater opened by excavation and downward displacement of materials at the center of the impact (Melosh, 1989; Melosh and Ivanov, 1999; Morgan and others, 2000). The stratabound collapse structure seen on the Langley seismic images is interpreted as representative of this late stage of impact crater evolution.

Exmore Beds

During impacts into marine targets, late-stage gravitational collapse may be accompanied or closely followed by the catastrophic resurge of water-sediment-ejecta mixtures into the collapsing crater, resulting in local erosion and extensive sediment deposition (Tsikalas and others, 1998; Ormö and Lindström, 2000; von Dalwigk and Ormö, 2001; Shuvalov and others, 2002; Tsikalas and Faleide, 2002). The Exmore beds in the Langley core display vertical variations in fossil assemblages and lithoclast size and composition that suggest two depositional units with different provenances produced by resurge sedimentation (Frederiksen and others, this volume, chap. D; Gohn and others, this volume, chap. C). Two of the four seismically defined subunits of the Exmore beds shown on the migrated depth image (figs. I9 and I11) likely represent the depositional units observed in the core.

The base of seismic subunit 4 of the Exmore beds is a strong, continuous reflection located at about 250 m to 245 m (820 ft to 804 ft) depth near the Langley corehole (fig. I9). Gohn and others (this volume, chap. C) recognize a depositional boundary at about 244 m (about 800 ft) depth in the core on the basis of size grading (coarse-tail-grading) of the larger lithoclasts. Frederiksen and others (this volume, chap. D) note that reworked Cretaceous calcareous nannofossils are present in the Exmore matrix only at and above 242.1 m (794.4 ft) depth, suggesting differences in sediment sources for the deposits above and below that sample depth. The close proximity in depth of these three boundaries suggests the correlation of the two depositional units defined in the core with Exmore subunits 2 and 4 interpreted on the migrated depth image (fig. I11).

The upper contact of the Exmore beds is a wavy, nearly continuous reflection with about 10 m (33 ft) of relief, as seen on the migrated depth image (figs. I9 and I11). We speculate that this irregular surface may represent large bedforms, either megaripples or hummock-and-swale bed topography. These features could have resulted from low-density ocean-resurge currents or wave-interference patterns produced by collapse of the transient water-column crater or by the return of impact-generated tsunamis from the nearby North American shoreline. Alternatively, this irregular surface may represent the essentially unmodified hummocky or blocky upper surface of the final Exmore debris flow (for non-impact examples, see Prior and others, 1984, and Mulder and Cochonat, 1996). Wavy reflections in the postimpact Chickahominy Formation may represent the draping of fine-grained marine sediments over the irregular upper surface of the Exmore beds.

Summary

Complementary data from the seismic reflection and refraction survey and the corehole at the NASA Langley Research Center allowed us to describe and interpret the stratigraphy and impact deformation of preimpact rocks and sediments and the deposition of synimpact sediments within part of the annular trough of the Chesapeake Bay impact structure. A stratabound collapse structure within the preimpact sedimentary section of the annular trough is interpreted to have formed during widespread, late-stage gravitational collapse of the impact structure. Observed deformation features increase upward in the preimpact section, including fracturing of clays, fluidization of sands, and injection of previously overlying Upper Cretaceous and Tertiary marine sediments. Fluidized sands within the lower part of the sedimentary section probably provided a detachment interval and accommodation space in the lower part of the collapse structure. The Exmore beds are interpreted as ocean-resurge deposits that consist of multiple depositional units with differing provenances. Resurge currents or returning impact-generated tsunamis may have modified the upper surface of the Exmore beds.

Acknowledgments

U.S. Geological Survey (USGS) investigations of the Chesapeake Bay impact structure are conducted in cooperation with the Hampton Roads Planning District Commission, the Virginia Department of Environmental Quality, and the National Aeronautics and Space Administration (NASA) Langley Research Center. The Hampton Roads Planning District Commission and the USGS provided funds for the drilling of the USGS-NASA Langley corehole. The Virginia Department of Environmental Quality and the Department of Geology of the College of William and Mary provided extensive operational support at the drill site. The NASA Langley Research Center provided extensive operational and logistical support for the drilling of the USGS-NASA Langley corehole and for the York-James seismic survey. We especially thank Joel S. Levine, John J. Warhol, Jr., and Frederick M. Thompson (all of NASA-Langley), for their enthusiastic support during these operations.

We thank Dominion Virginia Power for access to their right-of-way in Hampton and Newport News. We also thank the members of the USGS seismic field crew, whose hard work and dedication made this research possible: Joe Catchings, Chris Crosby, Gini Gandhok, Shawn Hanson, Ron Kaderabek, Bryan Kerr, Lora Kiger, Colleen McCartan, Lela Preshad, Jose Rodriguez, Ben Sleeter, and Matthew Smith. The USGS Rocky Mountain Drilling Unit (Arthur C. Clark, supervisor and lead driller) drilled the USGS-NASA Langley corehole with support from the USGS Eastern Earth Surface Processes Team's drilling crew. Stephen E. Curtin (USGS) and Richard E. Hodges (USGS) conducted the geophysical logging of the Langley corehole. We thank Nicholas M. Ratcliffe (USGS) and Thomas M. Brocher (USGS) for their reviews of this chapter, which substantially improved its organization and content.

References Cited

Anstey, N.A., 1977, Seismic interpretation; The physical aspects: Boston, International Human Resources Development Corporation, 637 p.

Barry, K.M., Cavers, D.A., and Kneale, C.W., 1975, Recommended standards for digital tape formats: Geophysics, v. 40, no. 2, p. 344–352.

Brouwer, Jan, and Helbig, Klaus, 1998, Shallow high-resolution reflection seismics, v. 19 *of* Helbig, Klaus, and Treitel, Sven, eds., Handbook of geophysical exploration; Section 1, Seismic exploration: New York, Elsevier, 391 p.

Edwards, L.E., and Powars, D.S., 2003, Impact damage to dinocysts from the late Eocene Chesapeake Bay event: Palaios, v. 18, no. 3, p. 275–285. (Also available online at http://www.bioone.org/pdfserv/i0883-1351-018-03-0275.pdf)

Gohn, G.S., Bruce, T.S., Catchings, R.D., Emry, S.R., Johnson, G.H., Levine, J.S., McFarland, E.R., Poag, C.W., and Powars, D.S., 2001, Integrated geologic, hydrologic, and geophysical investigations of the Chesapeake Bay impact structure, Virginia, USA; A multi-agency program [abs.]: Lunar and Planetary Science Conference, 32d, Houston, Tex., March 12–16, 2001, Abstract 1901, available online at http://www.lpi.usra.edu/meetings/lpsc2001/pdf/1901.pdf

Gohn, G.S., Clark, A.C., Queen, D.G., Levine, J.S., McFarland, E.R., and Powars, D.S., 2001, Operational summary for the USGS-NASA Langley corehole, Hampton, Virginia: U.S. Geological Survey Open-File Report 01–87–A, 21 p., available only online at http://pubs.usgs.gov/of/2001/of01-087/

Hole, J.A., 1992, Nonlinear high-resolution three-dimensional seismic travel time tomography: Journal of Geophysical Research, v. 97, no. B5, p. 6553–6562.

Melosh, H.J., 1989, Impact cratering—A geologic process: New York, Oxford University Press, 245 p.

Melosh, H.J., and Ivanov, B.A., 1999, Impact crater collapse: Annual Review of Earth and Planetary Sciences, v. 27, p. 385–415.

Morgan, J.V., Warner, M.R., Collins, G.S., Melosh, H.J., and Christeson, G.L., 2000, Peak-ring formation in large impact craters; Geophysical constraints from Chicxulub: Earth and Planetary Science Letters, v. 183, no. 3–4, p. 347–354.

Mulder, Thierry, and Cochonat, Pierre, 1996, Classification of offshore mass movements: Journal of Sedimentary Research, v. 66, no. 1, p. 43–57.

Olsson, R.K., Gibson, T.G., Hansen, H.J., and Owens, J.P., 1988, Geology of the northern Atlantic Coastal Plain; Long Island to Virginia, *in* Sheridan, R.E., and Grow, J.A., eds., The Atlantic continental margin, U.S., v. I–2 *of* The geology of North America: Boulder, Colo., Geological Society of America, p. 87–105.

Ormö, Jens, and Lindström, Maurits, 2000, When a cosmic impact strikes the sea bed: Geological Magazine, v. 137, no. 1, p. 67–80.

Poag, C.W., 1996, Structural outer rim of Chesapeake Bay impact crater; Seismic and bore hole evidence: Meteoritics & Planetary Science, v. 31, no. 2, p. 218–226.

Poag, C.W., 1997, The Chesapeake Bay bolide impact; A convulsive event in Atlantic Coastal Plain evolution: Sedimentary Geology, v. 108, no. 1–4, p. 45–90.

Poag, C.W., Hutchinson, D.R., Colman, S.M., and Lee, M.W., 1999, Seismic expression of the Chesapeake Bay impact crater; Structural and morphologic refinements based on new seismic data, *in* Dressler, B.O., and Sharpton, V.L., eds., Large meteorite impacts and planetary evolution; II: Geological Society of America Special Paper 339, p. 149–164.

Poag, C.W., Powars, D.S., Poppe, L.J., and Mixon, R.B., 1994, Meteoroid mayhem in Ole Virginny—Source of the North American tektite strewn field: Geology, v. 22, no. 8, p. 691–694.

Powars, D.S., 2000, The effects of the Chesapeake Bay impact crater on the geologic framework and the correlation of hydrogeologic units of southeastern Virginia, south of the James River: U.S. Geological Survey Professional Paper 1622, 53 p., 1 oversize pl. (Also available online at http://pubs.usgs.gov/prof/p1622)

Powars, D.S., and Bruce, T.S., 1999, The effects of the Chesapeake Bay impact crater on the geological framework and correlation of hydrogeologic units of the lower York-James Peninsula, Virginia: U.S. Geological Survey Professional Paper 1612, 82 p., 9 oversize pls. (Also available online at http://pubs.usgs.gov/prof/p1612)

Powars, D.S., Bruce, T.S., Bybell, L.M., Cronin, T.M., Edwards, L.E., Frederiksen, N.O., Gohn, G.S., Horton, J.W., Jr., Izett, G.A., Johnson, G.H., Levine, J.S., McFarland, E.R., Poag, C.W., Quick, J.E., Schindler, J.S., Self-Trail, J.M., Smith, M.J., Stamm, R.G., and Weems, R.E., 2001, Preliminary geologic summary for the USGS-NASA Langley corehole, Hampton, Virginia: U.S. Geological Survey Open-File Report 01–87–B, 20 p., available only online at http://pubs.usgs.gov/of/2001/of01-087/

Powars, D.S., Gohn, G.S., Catchings, R.D., Horton, J.W., Jr., and Edwards, L.E., 2003, Recent research in the Chesapeake Bay impact crater, USA—Part 1. Structure of the western annular trough and interpretation of multiple collapse structures [abs.]: International Conference on Large Meteorite Impacts, 3d, Noerdlingen, Germany, August 5–7, 2003, Abstract 4053, available online at http://www.lpi.usra.edu/meetings/largeimpacts2003/pdf/4053.pdf

Powars, D.S., Johnson, G.H., Edwards, L.E., Horton, J.W., Jr., Gohn, G.S., Catchings, R.D., McFarland, E.R., Izett, G.A., Bruce, T.S., Levine, J.S., and Pierce, H.A., 2002, An expanded Chesapeake Bay impact structure, eastern Virginia; New corehole and geophysical data [abs.]: Lunar and Planetary Science Conference, 33d, League City, Tex., March 11–15, 2002, Abstract 1034, available online at http://www.lpi.usra.edu/meetings/lpsc2002/pdf/1034.pdf

Powars, D.S., Mixon, R.B., and Bruce, Scott, 1992, Uppermost Mesozoic and Cenozoic geologic cross section, outer coastal plain of Virginia, *in* Gohn, G.S., ed., Proceedings of the 1988

U.S. Geological Survey Workshop on the Geology and Geohydrology of the Atlantic Coastal Plain: U.S. Geological Survey Circular 1059, p. 85–101.

Prior, D.B., Bornhold, B.D., and Johns, M.W., 1984, Depositional characteristics of a submarine debris flow: Journal of Geology, v. 92, no. 6, p. 707–727.

Shuvalov, V.V., Dypvik, H., and Tsikalas, F., 2002, Numerical modeling of the Mjølnir marine impact event [abs.]: Lunar and Planetary Science Conference, 33d, League City, Tex., March 11–15, 2002, Abstract 1038, available online at http://www.lpi.usra.edu/meetings/lpsc2002/pdf/1038.pdf

Stewart, S.A., and Allen, P.J., 2002, A 20-km-diameter multi-ringed impact structure in the North Sea: Nature, v. 418, no. 6897, p. 520–523.

Tsikalas, Filippos, and Faleide, J.I., 2002, Near-field erosional features at the Mjølnir impact crater; The role of marine sedimentary target [abs.]: Lunar and Planetary Science Conference, 33d, League City, Tex., March 11–15, 2002, Abstract 1296, available online at http://www.lpi.usra.edu/meetings/lpsc2002/pdf/1296.pdf

Tsikalas, Filippos, Gudlaugsson, S.T., and Faleide, J.I., 1998, Collapse, infilling, and postimpact deformation at the Mjølnir impact structure, Barents Sea: Geological Society of America Bulletin, v. 110, no. 5, p. 537–552.

von Dalwigk, Ilka, and Ormö, Jens, 2001, Formation of resurge gullies at impacts at sea; The Lockne crater, Sweden: Meteoritics & Planetary Science, v. 36, no. 3, p. 359–369.

Waters, K.H., 1981, Reflection seismology; A tool for energy resource exploration (2d ed.): New York, John Wiley and Sons, 453 p., 4 pls.